Harnessing Random Peptide Mixtures to Overcome Multidrug-Resistant Fungal Infections

John Adeoye[1], Yael Belo[2], Marina Rocha[1], Hilla Hayby[1], Zvi Hayouka[2], Neta Shlezinger[1]

[1] Koret School of Veterinary Medicine, Faculty of Agriculture, The Hebrew University, Rehovot, Israel

[2] Institute of Biochemistry, Food Science and Nutrition, The Robert H. Smith Faculty of Agriculture, Food and Environment, The Hebrew University of Jerusalem, Rehovot, Israel

Corresponding author: neta.shlezinger1@mail.huji.ac.il

Abstract

Invasive fungal infections, characterized by high mortality rates, present a growing health concern due to the limited spectrum of effective drugs, escalating numbers of immunocompromised patients, and the rapid emergence of drug resistance. Addressing this challenge requires alternative therapeutic strategies. Candidate drugs should fulfill key requirements to qualify for clinical use, including negligible host toxicity, high *in vitro* and *in vivo* antifungal activity, *in vivo* stability, and modes of actions that reduce the potential for the emergence of resistant strains. Antimicrobial peptides (AMPs) stand out as a promising class of compounds to combat antimicrobial resistance. Capitalizing on the unique characteristics of AMPs, we have developed a novel approach, to synthesize random peptide mixtures (RPMs) with robust bactericidal properties against drug-resistant bacteria. Here, we evaluate the antifungal potential of RPMs. Our findings demonstrate high potency of RPMs against *Candida auris*, a newly emerged multidrug-resistant human fungal pathogen. In vitro studies demonstrated the effective eradication of *C. auris* by FK20 RPMs, with scanning electron microscopy revealing substantial damage to the fungal outer membrane, while confocal microscopy confirms their ability to penetrate *C. auris* cells. Importantly, our study elucidates that FK20 RPMs effectively hinder the development of resistance in *C. auris*, as confirmed by experimental evolution assays. Moreover, a synergistic effect is observed when combining FK20 RPMs with the antifungal drug caspofungin, effectively inhibiting biofilm formation. Lastly, we demonstrate the significant therapeutic potential of FK20 RPM in a murine model of systemic candidiasis. Our findings underscore the promise of RPMs as novel, efficacious, and safe treatment for drug-resistant fungal infections.

Introduction

The surge in antimicrobial resistance poses a significant threat to public health [1]–[4].While attention has predominantly centered on pan-resistant bacteria, mounting apprehension surrounds multidrug-resistant fungal pathogens, notably *Candida auris*. This emerging pathogen poses a significant global health threat due to its rapid worldwide spread and intrinsic multidrug resistance [5], [6]. The U.S. Centers for Disease Control and Prevention classified C. auris as one of only five pathogens posing the most urgent threat to public health in their 2019 Antibiotic Resistance Threats Report [7], underscoring the necessity for additional therapeutic options to address drug-resistant fungal infections.

C. auris was initially identified in 2009 in a Japanese hospital, where it was isolated from the external ear canal of a patient [8]. Since then, genomic analysis has shed light on the concurrent emergence of distinct lineages, categorizing them into four major geographical clades across six continents over the past ~400 years [9], [10](ref). Its rapid transmission within clinical settings is attributed to its remarkable long-term persistence on surfaces, including human skin, as well as the widespread prevalence of drug resistant isolates (refs). Hospital-acquired *C. auris* infections, represented primarily by candidemia, typically ensue after skin colonization in patients, with mortality rates ranging from 30% to 60% [11], [12]. Risk factors that increase susceptibility to *C. auris* infections are shared with other fungal infections and include iatrogenic, primary, or acquired immunodeficiency, prolonged antibiotic regimens, prolonged hospitalization, and invasive medical procedures [13].

C. auris is classified as a 'superbug fungus', posing an increasingly concerning threat to human health due to varying levels of intrinsic resistance. Approximately 5-10% of isolates exhibit resistance to all three major antifungal drug classes commonly used in clinical settings [14], [15]. It is evident that over 80% of *C. auris* isolates are resistant to azole antifungals [11], and many strains exhibit notably elevated Minimum Inhibitory Concentrations (MIC) for polyenes such as Amphotericin B [16]–[18]. For these reasons, echinocandins such as caspofungin, are used as front-line therapeutics against systemic candidemia caused by *C. auris* [19]–[21]. However, *C. auris* isolates with a reduced susceptibility to one or more drugs in the echinocandin class have also been detected [11], [22], [23]. Similar to the other candida species, *C. auris* employs diverse drug resistance mechanisms, including genomic point mutations or large-scale chromosomal changes that alter drug targets, and duplications of efflux pumps or their regulators. Comprehensively, the coexisting features of multidrug resistance, rapid global emergence, and heightened mortality rates collectively designate *C. auris* as a pathogen of significant concern and complexity. Thus, there is an urgent need of developing new and sophisticated antifungals to fight against *C. auris*.

Antimicrobial peptides (AMPs) stand as integral components within the immune systems of diverse organisms [24]. Characterized by short sequences, these peptides are composed of cationic and hydrophobic residues, granting them a multifaceted spectrum of activity [25], [26]. Operating through non-specific mechanisms, AMPs play a pivotal role in immune defense by disrupting membrane integrity through the formation of pores in invading pathogens [27]. Building on the principles of AMPs, we have innovated the development of a novel class of antimicrobial peptides known as Random Peptide Mixtures (RPMs). Our approach involves the solid-phase synthesis of these peptides, where each coupling step introduces a mix of two amino acids, one cationic and one hydrophobic [28]. This method imparts increased variability, while preserving peptides' defined chain length, stereochemistry and overall composition. RPMs have exhibited remarkable antimicrobial efficacy against both Gram-positive and Gram-negative bacteria [29]–[33]. Here, we present for the first time, the potential of RPMs as antifungal drugs against the challenging fungal pathogen *C. auris*.

Results

Random Peptide Mixtures Demonstrate Strong Antifungal Activity against *C. auris* In Vitro

We initiated our study by comparing the antifungal activity of various RPMs against *C. auris* through a series of killing assays. We began with a comparison of RPMs based on their amino acid composition. Notably, among the tested RPMs, FK20 (L-Phenylalanine−L-Lysine, 20-mer) exhibited superior antifungal activity when compared to the LK20 RPM (L-Leucine−L-Lysine, 20- mer) (Figure 1A). As part of our screening process, we evaluated the efficacy of IK20 and IK10 RPMs (L-Isoleucine−L-Lysine, 20-mer and 10-mer), both of which displayed minimal activity against *C. auris*. Consequently, these RPMs were chosen as negative control RPMs. We proceeded to examine the efficacy of FK RPMs with varying chain lengths (Figure 1B). Among these, the 5 and 10-mer FK RPMs did not exhibit any discernible antifungal properties, while the 30-mer FK RPM displayed only marginal activity. Notably, the FK20 RPM demonstrated the most substantial antifungal activity, consistent with our findings regarding antibacterial activity [34]. Subsequently, we explored the impact of FK RPM stereochemistry (Figure 1C). Our analysis involved three variants: FK20 (L-Phenylalanine−L-Lysine, 20-mer), FdK20 (L-Phenylalanine−D-Lysine, 20-mer), and dFdK20 (D-Phenylalanine−D-Lysine, 20-mer). Interestingly, the two homochiral RPMs, FK20 and dFdK20, exhibited robust antifungal activity, while the hetrochiral RPM FdK20 displayed comparatively lower activity levels. Furthermore, we investigated the activity of 5-mer FK RPMs that were conjugated to palmitic acid (Figure 1D). These 5-mer FK RPMs demonstrated

limited antifungal activity. Upon careful consideration of these results, we identified FK20 homochiral RPMs as the most effective candidates for combating *C. auris*. Consequently, we selected these RPMs for all subsequent experiments.

Characterization of *C. auris* Eradication by FK20 RPMs

We first examined the ability of FK20 RPM to penetrate *C. auris* cells. For this purpose we have synthesized FK20 RPM and labeled the N' terminus free amino group with 5(6)-carboxyfluorescein. *C. auris* cells were visualized by confocal microscope after 45 min incubation together with the fluorescently labeled FK20, followed by Calcofluor White staining (Figure 2). We could visualize the fluorescein labeled FK20 RPM (green) inside *C. auris* cells, as it surrounded by the Calcofluor White labeled *C. auris* cell walls (blue) [Video 1]. We assume that part of the RPM caused damage to the fungi outer surface, and enhanced the entry of other peptide molecules into the *C. auris* cells. In order to examine the outer surface of *C. auris* after interaction with FK20 RPMs, we performed a Scanning Electron Microscopy (SEM) study. *C.auris* cells were incubated together with 200 µg/mL of the different FK20 RPMs and visualized by SEM (Figure 3). According to our findings, the homochiral peptide mixtures, FK20 and dFdK20 were able to efficiently form damage in the outer surface of *C. auris* cells, compared to the hetrochiral peptide mixture FdK20. We also observed massive aggregation while using the homochiral peptide mixtures, compared to the control sample. To further characterize the impact of FK20 RPM on the integrity of the *C. auris* outer surface, we employed Propidium Iodide (PI). PI, a fluorescent dye widely utilized for nucleic acid staining, particularly DNA, serves as a reliable marker to differentiate between live and dead cells within a population [35]. Due to its impermeability to intact cell membranes, PI is commonly used to highlight cells with compromised or damaged membranes [36]. A killing assay was conducted, involving escalating concentrations of FK20, followed by PI staining and FACS analysis. The results revealed significant PI staining in a concentration-dependent manner, indicating an escalating level of membrane damage corresponding to the increasing concentrations of FK20 (Figure 4). Parallelly, the use of Ghost dye produced similar outcomes, further supporting our observations (Figure S1).

Random Peptide Mixtures Inhibit the Development of *C. auris* Resistance

To investigate the potential of *C. auris* to acquire resistance against FK20 RPM, we performed an *in vitro* experimental evolution in laboratory conditions according to established protocols with slight modifications [37] (Figure 5A). Briefly, we performed ten serial passages of *C. auris* cells in RPMI-1640 media containing 100 µg/mL FK20. This passage resulted in the emergence of three independently evolved FK20 outcome strains. We also performed in parallel an experimental evolution of *C. auris* to caspofungin, a known inducer of antifungal resistance in

C. auris yielding three independent caspofungin-evolved outcome strains. As a control, *C. auris* strains were equally passaged in RPMI-1640 media alone without antifungal agents resulting in no-drug-evolved strains (ND-Evol). Subsequently, all outcome strains from these experimental evolutions performed were systematically challenged with the respective antifungal agent specific to their evolutionary paths. Growth kinetics were monitored via measurement of end point absorbance after 72 hours to determine their new MIC-50 and were compared with MIC-50 values of the parental strains. We did not observe a significant change in the MIC-50 of FK20 evolved strains compared to the parental strains and the no-drug-evolved strains (Figure 5B). In contrast there was a rapid increase in the MIC-50 of caspofungin evolved strains to >10 µg/mL (Figure 5C). These results indicate that while *C. auris* cells may rapidly evolve to develop antifungal resistance to caspofungin within 10 passages, FK20-Evolved strains failed to develop antifungal resistance to FK20 RPM within the same evolution time frame.

Collateral sensitivity is seen as an evolutionary trade-off mechanism in which the acquisition of resistance towards an antibiotic or antifungal drug produces increased susceptibility to another antibiotic or antifungal agent [38]. In light of this, we evaluated the resistance profiles of FK20-evolved strains and caspofungin-evolved strains when systematically challenged with the reciprocal antifungal agents with which experimental evolution was performed, i.e., caspofungin and FK20, respectively. We observed that FK20-evolved strains do not show significant differences in MIC-50 compared to parental and no-drug evolved strains when challenged with Caspofungin (Figure 5D). While caspofungin-evolved strains show a remarkable reduction in MIC-50 when exposed to FK20 RPM (Figure 5E). Indicating that while the development of resistance in FK20-evolved strains remain unaffected by caspofungin, caspofungin-evolved strains show increased collateral sensitivity to FK20-RPM.

FK RPM and Caspofungin are Synergistic and Inhibit *C. auris* Biofilm Formation

Inspired by the evolution experiment, we were curious to examine whether caspofungin and FK20 have synergistic properties. We have found out that FK20 cause damage to the outer surface of *C. auris* cells through interaction with their cell walls and membranes. Furthermore, caspofungin is an inhibitor of the enzyme (1→3)-β-D-glucan synthase and thereby disturbing the integrity of the fungal cell wall [39]. We hypothesize that their combination would induce multi cell wall damage, as they will be synergistic. We evaluated the combinatorial effect of FK20 and caspofungin on *C. auris* cells by challenging cells with FK20 (0-200 µg/mL) and caspofungin (0-3.2 µg/mL) using a checkerboard assay. We observed MIC-50 of combinations of FK20 and caspofungin to be 3.125 µg/mL and 1.05 µg/mL respectively (Figure 6A). We determined the nature of interaction by calculating the fractional inhibitory concentration index

(FICI) method [40]. FICI value was calculated to be 0.378 indicating a synergistic interaction between FK20 RPM and caspofungin.

Caspofungin demonstrates limited efficacy in addressing *C. auris* biofilms, with concentrations needed for complete inhibition exceeding safe levels for patient administration (requiring >32 µg/mL to inhibit 90% of biofilm formation) [41], [42]. Considering this, we explored the potential synergistic effects of the FK20 RPM and caspofungin, considering their combined use for biofilm inhibition. To assess this, a biofilm inhibition assay was conducted by culturing *C. auris* cells on a polystyrene 96-well plate with varying concentrations of FK20, Caspofungin, and their combinations. After 24 hours of incubation, the supernatant was removed, and the resulting biofilms were quantified using MTT and crystal violet separately (Figure 6B&C). Both caspofungin and FK20 exhibited a decrease in biofilm levels as drug concentrations increased. Caspofungin achieved complete biofilm formation inhibition at 12.8 µg/mL, as determined by MTT quantification. Meanwhile, FK20 required a concentration of 200 µg/mL for complete biofilm inhibition, according to crystal violet quantification. Notably, neither FK20 nor caspofungin individually inhibited biofilm formation at low concentrations. However, when combined at low concentrations in four different combinations, they collectively resulted in complete inhibition of biofilm formation. These findings underscore the high efficacy of caspofungin and FK20 combinations in inhibiting *C. auris* biofilm formation.

Random Peptide Mixtures Pose No Adverse Toxic Effects in Mice and Exhibit No Cytotoxicity in Cultured Cells and

To evaluate the in vitro safety profile of both RPMs, toxicity assays were conducted on RAW 264.7 murine macrophage cells. Incubating cells with varying concentrations of each RPM for 24 hours, viability was assessed using the MTT reagent. Results indicate that the tested 10-mer and 20-mer IK RPMs can be safely utilized at concentrations up to 400 µg/mL, while the FK20 RPM can be employed at up to 200 µg/mL for treating *C. auris* [Figure S2]. It's reasonable to consider that even higher concentrations may be safe, given the heightened sensitivity of *in vitro* and cell culture assays compared to the exposure of entire organisms to these compounds at residual concentrations. To comprehensively establish the safety of FK20 in vivo, a control group of mice received intramuscular daily administrations of ultra-pure water (UPW), FK20, or IK10 for four days (25 µg/gr body weight). On the fourth day, blood chemistry and hematology were analyzed. No significant differences were observed between the mouse cohorts treated with FK20 and PBS, evident in both in vitro hematology and blood chemistry profiles (Table S1). Furthermore, low hemolysis values were exhibited for both RPM treatments (Figure S3).

RPM Efficacy in Mouse Model of Candidiasis

We conducted a comprehensive examination of the therapeutic potential of FK20 in murine models infected with systemic candidiasis caused by *C. auris*. Immunosuppressed mice, induced through cyclophosphamide, were subjected to *C. auris* challenge, followed by daily treatment via intra-muscular administration of FK20 RPM at a dose of 25 µg/gr body weight. It is noteworthy that FK20 RPM had previously demonstrated both stability and systemic distribution over a 24-hour period [30]. As a control group, mice were subjected to treatment with IK RPMs, which lacked any discernible antifungal activity. Assessment of disease severity and survival, conducted four days post-infection, unveiled a notable reduction in clinical scores, an elevated survival percentage, and diminished weight loss in mice receiving FK20 RPM compared to their counterparts treated with IK RPMs [Figure 7B-D]. Although not reaching statistical significance, the fungal burden in the kidneys exhibited a marked decrease with FK20 RPM treatment in comparison to IK RPMs [Figure 7E]. In summary, our findings collectively underscore the efficacy of FK20 RPMs in mitigating acute infection in mouse models of candidiasis. The discernible reduction in disease severity, increased survival rates, and alleviated weight loss point towards the promising therapeutic potential of FK20 in the context of systemic candidiasis.

Discussion

In our study, we compared the antifungal activity of various RPMs against *C. auris*, revealing that FK20 exhibited superior antifungal properties compared to other RPMs. Subsequently, FK20 homochiral RPMs were identified as the most effective candidates for combating *Candida auris*, guiding our selection for further experiments. Investigating the penetration of FK20 RPM into *C. auris* cells, fluorescence imaging revealed internalization, suggesting potential damage to the fungal outer surface. Scanning Electron Microscopy (SEM) demonstrated efficient damage formation by homochiral peptide mixtures (FK20 and dFdK20) compared to the hetrochiral peptide mixture (FdK20). Further assessment using PI confirmed concentration-dependent membrane damage, supporting the observed effects on *C. auris* outer surface integrity. In an in vitro experimental evolution study, *C. auris* was exposed to FK20 RPM and caspofungin, resulting in caspofungin-evolved strains displaying a rapid increase in MIC-50, indicative of resistance development. In contrast, FK20-evolved strains showed no significant change in MIC-50, suggesting resistance did not develop. When challenged with reciprocal antifungal agents, FK20-evolved strains exhibited a consistent resistance profile, while caspofungin-evolved strains demonstrated increased collateral sensitivity to FK20 RPM, highlighting the potential of FK20 as a resilient antifungal agent against *C. auris*. Inspired by the evolution experiment, we investigated the synergistic properties of FK20 and caspofungin against *C. auris*. FK20 demonstrated damage to the fungal outer surface, while caspofungin disrupted the cell wall integrity. The combination showed a synergistic effect, as evidenced by

a significant reduction in MIC-50 values and successful inhibition of *C. auris* biofilm formation, highlighting the potential therapeutic efficacy of their combined use. In vitro toxicity assays showed that 10-mer and 20-mer IK RPMs are safe up to 400 µg/mL, and FK20 RPM up to 200 µg/mL for *C. auris* treatment. In vivo studies in mice demonstrated the safety of FK20 with no significant adverse effects on blood chemistry and hematology, supporting its overall safety profile. In conclusion, our study demonstrates the remarkable therapeutic efficacy of FK20 RPMs in reducing acute infection in murine models of systemic candidiasis caused by *C. auris*, as evidenced by significantly lower clinical scores, higher survival rates, and diminished weight loss compared to control IK RPM-treated mice.

Materials and Methods

Peptide Synthesis

Peptides were synthesized by a standard Fmoc-based solid-phase peptide synthesis (SPPS) on Rink Amide resin (substitution 0.6 mmol/gr), using a peptide synthesizer (Liberty Blue). Amino acids were diluted with dimethylformamide (DMF) to a final concentration of 0.2 M. Before coupling execution, 4 equivalents of amino acids were activated in DMF using 4 equiv. of DIC and 8 equiv. Oxyma. Fmoc deprotection step was conducted by 20% piperidine in DMF. At the end of the synthesis, the peptide mixtures were cleaved from the resin by adding a solution containing 95% trifluoroacetic acid (TFA), 2.5% double-distilled water (DDW) and 2.5% triisopropylsilane (TIPS) and stirred for 3 hours. The mixture was then filtered, and the peptides precipitated by the addition of 40 mL cold diethyl ether to the TFA solution and centrifuged. The supernatant was then removed and the peptide pellet dried, dissolved in 20% acetonitrile in DDW, frozen with liquid nitrogen and lyophilized. The synthesis was validated by MALDI-TOF mass spectrometry.

Cells and Reagents

Mouse macrophage-like RAW 264.7 cells were cultured in DMEM medium supplemented with 10% fetal bovine serum, 1% glutamine, 100 units/ml penicillin/streptomycin and maintained at 37°C in % CO_2. Toxicity assay was done using 3-(4, 5,-dimethyl thiazolyl-2)-2,5-diphenyl tetrazolium bromide assay (MTT).

C. auris Killing Assay

Overnight starter of *C. auris* was prepared in 5mL of YPD media, and grew at 37°C, 200 rpm. In the morning after, the starter was washed three times with PBS. Cells were counted using haemocytometer cell counter and the original starter was diluted with PBS. 10^6 cells/mL were incubated with 50 or 200 µg/mL of each RPM separately for 45 min at 37°C, 200 RPM in PBS.

The microbial burden was calculated after dilutions and plating each sample on YPD agar plates.

Mice, Animal Care, and Ethics Statement

All experiments involving the use of mice were approved by and performed according to the Hebrew University of Jerusalem Institutional Animal Care and Use Committee (IACUC) (protocol number MD-21-16494-5). The Hebrew University of Jerusalem is accredited by the NIH and by AAALAC to perform experiments on laboratory animals (NIH approval number: OPRR-A01-5011). Eight-week-old C57BL/6JOlaHsd female mice (18-20g) mice were purchased from Envigo, Israel. Mice were housed under specific pathogen-free conditions ingroups of five in individually ventilated cages with unrestricted access to food and water.

Murine Model of Systemic Candidiasis

Mice were immunosuppressed by intra-peritoneal injection of 0.2ml cyclophosphamide in PBS at 150 mg/kg three days before infection, 100mg/kg one day before infection, and two days post-infection. Infection inoculum was obtained by sub culturing *Candida auris* on agar plates grown at 37°C for 24h. Single colonies of *C. auris* were resuspended in PBS and adjusted to specified concentrations. Immunosuppressed mice were infected with 1 x 10^6 CFUs in 0.1 mL of PBS *via* the lateral tail vein injection. Treatment of mice with 25 µg/gr body weight of each RPM was initiated approximately 2 hours after infection, and repeated daily. Following infection, the health status and survival of mice were monitored daily. Clinical scores were assigned to each mouse to evaluate disease severity using disease severity indices obtained from observations of mice activity, grooming, lethargy, and posture. Mice showing severe signs of disease were humanely euthanized. The survival curves were analyzed by log-rank (Mantel-Cox) test using GraphPad Prism software version 8.00 (GraphPad Software, USA). Mice were sacrificed and the excised kidneys were weighed followed by homogenization using GentleMACS Dissociator (Miltenyi Biotec). Subsequently, 100 µL of the organ homogenate was used in the determination of CFUs following a 1:10000 dilution.

Determination of MIC

Minimum Inhibitory Concentration (MIC) assays for *Candida auris* B11117 strains were performed for FK20 and caspofungin according to European Committee on Antibiotic Susceptibility Testing (EUCAST) guidelines for determination of MIC using broth microdilution method [43], [44]. Single colonies were obtained for *Candida auris* B1117 strains streaked on Sabouraud Dextrose Agar (40 gr/L Dextrose, 10 gr/L Peptone, at pH 5.6) plates at 37°C for 24h. Approximately 1 x 10^5 *C. auris* cells were incubated in 200ul filter sterilized RPMI-1640 culture media (Sigma), supplemented with 1.8% glucose to reach a final

concentration of 2% and 0.03% L-Glutamine at pH 7.0. The growth media was supplemented with serial dilutions of antifungal agents 0 to 400 µg/mL of FK20 RPM, and 0 to 64 µg/ml of caspofungin in different 96-well microtiter plates. Cells were incubated in 96-well microtiter plates at 37°C and MIC was determined spectrophotometrically after 72h using Tecan Infinite M Plex plate reader (Neotec Bio, Israel).

Drug Combination Assay and Determination of Fractional Inhibitory Concentration

The determination of antifungal combination activity between caspofungin and FK20 was conducted using a checkerboard assay, followed by the calculation of the Fractional Inhibitory Concentration Index (FICI). Caspofungin and FK20 were individually added to each well at a volume of 50 µL, containing a four-fold strength of concentration. The final concentrations achieved in each well for caspofungin ranged from 0 to 3.2 µg/mL, while FK20 concentrations varied from 0 to 200 µg/mL. The yeast inoculum, consisting of 1 x 10^5 cells per well, was subsequently introduced into the plates. Plates were then incubated at 37°C for a duration of 72 hours. The antifungal combination activities of caspofungin and FK20 were assessed based on their FICI. The FICI was derived from the Inhibitory Concentration (IC-50), representing the inhibitory concentration at which 50% of the cell population are killed by the effect of the drug combination. The FICI was determined by the formula; $index = FIC_A + FIC_B = \frac{[A]}{MIC_A} + \frac{[B]}{MIC_B}$, where [A] and [B] are concentrations of drugs A and B, and MIC_A and MIC_B are their respective MIC values for *C. auris*. Synergy is significant if FICI ≤ 0.5, partial synergy if 0.5 < FICI ≤ 0.75, additive if 0.75 < FICI ≤ 1, indifferent if 1 < FICI ≤ 4, and antagonistic if FICI > 4.

Biofilm Formation and Quantification

In a 96-well microtiter plate, 200 µL of *C. auris* cells at a concentration of 10^6 CFU/mL were cultured in RPMI-1640 medium, supplemented with L-Glutamine (1%) and glucose (2%) for 24 hours at 37ºC together with different concentrations of a FK20, caspofungin, or combinations that were tested to study their effects on biofilm formation. Inhibition of biofilm formation was assessed using a crystal violet assay. Planktonic cells were removed, mature biofilms were washed with DDW, and then stained with 125 µL of 0.1% crystal violet for 15 minutes. Excess stain was washed off, and the biofilms were air-dried for 4 hours at 25ºC. Finally, they were re-stained with 125 µL of 30% acetic acid and biofilm biomass was quantified at 595 nm using a microplate reader (Tecan infinite M200). Biofilm formation was also assessed using the 3-(4,5-dimethylthiazol-2)-2,5-diphenyltetrazolium bromide (MTT) assay. In this method, each well was loaded with 50 µL of MTT reagent (1.5 mg/mL), and the plate was incubated for 1.5 hours at 37ºC. Subsequently, 150 µL of dimethyl sulfoxide (DMSO)

was added, and the plate was incubated for 10 minutes at 30ºC with agitation at 180 RPM. The absorbance was then measured at 595 nm using a TECAN Infinite plate reader.

In vitro experimental evolution

In vitro experimental evolution for *Candida auris* was performed according to the protocol published in with minor modifications [37]. Briefly, *Candida auris* B11117 was evolved in 100 µg/mL of FK20 RPM and 2 µg/mL of caspofungin. *C. auris* was also passaged simultaneously without exposure to any antifungal drug. The concentration of FK20 RPM selected for the experimental evolution was equivalent to the predetermined MIC_{50} of the parental *C. auris* B11117 strain. The experimental evolution was initiated by generating three independent replicates of *C. auris* B11117 as the parental strain. Cultures were struck from frozen parental stocks onto Sabouraud Dextrose Agar (40 gr/L Dextrose, 10 gr/L Peptone, at pH 5.6) plates and incubated at 37°C overnight. Each parental replicate was generated from randomly selected single colonies. Subcultures were made in YPD liquid media and incubated at 37°C overnight at 100 rpm. The overnight culture was diluted 1: 1000 in RPMI-1640 (supplemented with 1.8% glucose to reach a final concentration of 2% glucose and 0.03% L-Glutamine at pH 7.0) to a final volume of 1 mL. RPMI-1640 media was supplemented with 100µg/ml of FK20 and 2.5 µg/mL of caspofungin for replicates evolved with FK20 and caspofungin respectively, and supplemented RPMI-1640 media for replicates evolved without drugs in 96-deep well plates and incubated at 37°C for 72 hr. From cultures of each replicate, 100 µL of each replicate was frozen in 25% glycerol as parental replicates at time zero. Precautions were taken to minimize contaminations while keeping environmental conditions similar. Plates were sealed with gas-permeable membranes to allow gas exchange and maximum growth. The 96-deep well plate was incubated at 37°C without shaking to mimic static growth used in clinical resistance assays. Plates were incubated in plastic trays lined with wet paper towels to minimize evaporation. Following incubation for 72 hr, individual wells were mixed by pipetting and diluted 1:100 into fresh RPMI-1640 supplemented with or without drugs. In total 10 transfers were carried out, and 100 µL of evolved replicate cultures were frozen in duplicates in 25% glycerol for each transfer until after the tenth transfer and maintained at -80°C.

Determination of Resistance for Evolved Strains

Initial susceptibility of all parental strains was tested using broth microdilution liquid assays to determine the MIC_{50} that is, the concentration of antifungal agent at which 50 percent of the cell population are eliminated. The liquid assay experiment was carried out according to cell dilution regulations of the European Committee on Antibiotic Susceptibility Testing (EUCAST) guidelines with some modifications [43], [44]. Briefly, RPMI incubated at 37°C was used at the base media, and growth was determined as absorbance of cell densities at OD_{590}

at 24, 48, and 72 hr post-inoculation. MIC_{50} was numerically calculated as the concentration in which a 50% decrease in turbidity was determined spectrophotometrically.

Viability Staining

To assess the fungicidal activity of FK20, approximately 1 x 10^6 cells/mL were incubated with varying concentrations of FK20, ranging from 0 to 400 µg/mL for 45 minutes at 37C with continuous shaking. Subsequently, treated cells were washed with PBS and resuspended with either Propidium Iodide (BioLegend) or Ghost-Dye (Tonbo Biosciences) viability stain for 20 minutes. Residual viability dyes were washed with PBS, and cells were resuspended in PBS for analysis of fluorescence by flow cytometer.

References

[1] D. Chinemerem Nwobodo *et al.*, "Antibiotic resistance: The challenges and some emerging strategies for tackling a global menace," *J. Clin. Lab. Anal.*, vol. 36, no. 9, pp. 1–10, 2022.

[2] C. J. Murray *et al.*, "Global burden of bacterial antimicrobial resistance in 2019: a systematic analysis," *Lancet*, vol. 399, no. 10325, pp. 629–655, 2022.

[3] Z. Zhang *et al.*, "Assessment of global health risk of antibiotic resistance genes," *Nat. Commun.*, vol. 13, no. 1, 2022.

[4] R. E. Nelson *et al.*, "National estimates of healthcare costs associated with multidrug-resistant bacterial infections among hospitalized patients in the United States," *Clin. Infect. Dis.*, vol. 72, no. Suppl 1, pp. S17–S26, 2021.

[5] M. V. Horton, A. M. Holt, and J. E. Nett, "Mechanisms of pathogenicity for the emerging fungus Candida auris," *PLoS Pathog.*, vol. 19, no. 12 December, pp. 1–18, 2023.

[6] M. L. Cristina *et al.*, "An Overview on Candida auris in Healthcare Settings," *J. Fungi*, vol. 9, no. 9, p. 913, 2023.

[7] Centers for Disease Control and Prevention, "Antibiotic Resistance Threats in The United States 2019," *Antibiot. Resist. Threat. United States (U.S. Dep. Heal. Hum. Serv.*, vol. 10, no. 1, 2019.

[8] K. Satoh, K. Makimura, Y. Hasumi, Y. Nishiyama, K. Uchida, and H. Yamaguchi, "Candida auris sp. nov., a novel ascomycetous yeast isolated from the external ear canal of an inpatient in a Japanese hospital," *Microbiol. Immunol.*, vol. 53, no. 1, pp. 41–44, 2009.

[9] J. Rhodes and M. C. Fisher, "Global epidemiology of emerging Candida auris," *Curr. Opin. Microbiol.*, vol. 52, pp. 84–89, 2019.

[10] S. R. Lockhart, R. Adam, A. Alanio, A. Alastruey-izquierdo, S. Althawadi, and B. Araúz, "Tracing the Evolutionary History and Global Expansion of Candida auris Using Population Genomic Analyses," *MBio*, vol. 11, no. 2, 2020.

[11] S. R. Lockhart *et al.*, "Simultaneous emergence of multidrug-resistant candida auris on 3 continents confirmed by whole-genome sequencing and epidemiological analyses," *Clin. Infect. Dis.*, vol. 64, no. 2, pp. 134–140, 2017.

[12] K. Arensman *et al.*, "Clinical Outcomes of Patients Treated for Candida auris Infections in a Multisite Health System, Illinois, USA," *Emerg. Infect. Dis.*, vol. 26, no. 5, pp. 866–871, 2020.

[13] P. Jangir, S. Kalra, S. Tanwar, and V. K. Bari, “Azole resistance in Candida auris: mechanisms and combinatorial therapy,” *Apmis*, vol. 131, no. 8, pp. 442–462, 2023.
[14] J. Chen *et al.*, “Is the superbug fungus really so scary? A systematic review and meta-analysis of global epidemiology and mortality of Candida auris,” *BMC Infect. Dis.*, vol. 20, no. 1, pp. 1–10, 2020.
[15] J. Tu *et al.*, “Discovery of a new chemical scaffold for the treatment of superbug Candida auris infections,” *Emerg. Microbes Infect.*, vol. 12, no. 1, 2023.
[16] A. Chowdhary *et al.*, “A multicentre study of antifungal susceptibility patterns among 350 Candida auris isolates (2009-17) in India: Role of the ERG11 and FKS1 genes in azole and echinocandin resistance,” *J. Antimicrob. Chemother.*, vol. 73, no. 4, pp. 891–899, 2018.
[17] F. Chaabane, A. Graf, L. Jequier, and A. T. Coste, “Review on Antifungal Resistance Mechanisms in the Emerging Pathogen Candida auris,” *Front. Microbiol.*, vol. 10, no. November, pp. 1–8, 2019.
[18] A. Sanyaolu *et al.*, “Candida auris: An Overview of the Emerging Drug-Resistant Fungal Infection,” *Infect. Chemother.*, vol. 54, no. 2, pp. 236–246, 2022.
[19] A. Chowdhary, A. Voss, and J. F. Meis, “Multidrug-resistant Candida auris: ‘new kid on the block’ in hospital-associated infections?,” *J. Hosp. Infect.*, vol. 94, no. 3, pp. 209–212, 2016.
[20] S. Hu *et al.*, “Retrospective Analysis of the Clinical Characteristics of Candida auris Infection Worldwide From 2009 to 2020,” *Front. Microbiol.*, vol. 12, no. May, pp. 1–9, 2021.
[21] N. Geremia, P. Brugnaro, M. Solinas, C. Scarparo, and S. Panese, “Candida auris as an Emergent Public Health Problem: A Current Update on European Outbreaks and Cases,” *Healthc.*, vol. 11, no. 3, pp. 1–12, 2023.
[22] A. Chowdhary *et al.*, “Multidrug-resistant endemic clonal strain of Candida auris in India,” *Eur. J. Clin. Microbiol. Infect. Dis.*, vol. 33, no. 6, pp. 919–926, 2014.
[23] M. C. Arendrup, A. Prakash, J. Metetiadis, C. Sharma, and A. Chowdhary, “Comparison of EUCAST and CLSI Reference Microdilution MICs of Eight and Associated Tentative,” *Antimicrob. Agents Chemother.*, vol. 61, no. 6, pp. 1–10, 2017.
[24] Y. Huan, Q. Kong, H. Mou, and H. Yi, “Antimicrobial Peptides: Classification, Design, Application and Research Progress in Multiple Fields,” *Front. Microbiol.*, vol. 11, no. October, pp. 1–21, 2020.
[25] J. M. Ageitos, A. Sánchez-Pérez, P. Calo-Mata, and T. G. Villa, “Antimicrobial peptides (AMPs): Ancient compounds that represent novel weapons in the fight against bacteria,” *Biochem. Pharmacol.*, vol. 133, pp. 117–138, 2017.
[26] P. Kumar, J. N. Kizhakkedathu, and S. K. Straus, “Antimicrobial peptides: Diversity, mechanism of action and strategies to improve the activity and biocompatibility in vivo,” *Biomolecules*, vol. 8, no. 1, 2018.
[27] L. E. Reddick and N. M. Alto, “Bacteria fighting back: How pathogens target and subvert the host innate immune system,” *Mol. Cell*, vol. 54, no. 2, pp. 321–328, 2014.
[28] Z. Amso and Z. Hayouka, “Antimicrobial random peptide cocktails: A new approach to fight pathogenic bacteria,” *Chem. Commun.*, vol. 55, no. 14, pp. 2007–2014, 2019.
[29] T. Stern, E. Zelinger, and Z. Hayouka, “Random peptide mixtures inhibit and eradicate methicillin-resistant: Staphylococcus aureus biofilms,” *Chem. Commun.*, vol. 52, no. 44, pp. 7102–7105, 2016.
[30] R. C. Bennett *et al.*, “Random Peptide Mixtures as Safe and Effective Antimicrobials against Pseudomonas aeruginosa and MRSA in Mouse Models of Bacteremia and Pneumonia,” *ACS Infect. Dis.*, vol. 7, no. 3, pp. 672–680, 2021.
[31] S. Topman *et al.*, “Random peptide mixtures as new crop protection agents,” *Microb. Biotechnol.*, vol. 11, no. 6, pp. 1027–1036, 2018.
[32] J. Z. Lau *et al.*, “ Antibacterial efficacy of an ultra-short palmitoylated random peptide mixture in mouse models of infection by carbapenem-resistant Klebsiella pneumoniae ,” *Antimicrob. Agents Chemother.*, vol. 67, no. 11, pp. 1–18, 2023.
[33] H. Cheriker, T. Stern Bauer, Y. Oren, S. Nir, and Z. Hayouka, “Immobilized random

peptide mixtures exhibit broad antimicrobial activity with high selectivity," *Chem. Commun.*, vol. 56, no. 75, pp. 11022–11025, 2020.

[34] Z. Hayouka, S. Chakraborty, R. Liu, M. D. Boersma, B. Weisblum, and S. H. Gellman, "Interplay among subunit identity, subunit proportion, chain length, and stereochemistry in the activity profile of sequence-random peptide mixtures," *J. Am. Chem. Soc.*, vol. 135, no. 32, pp. 11748–11751, 2013.

[35] M. Rosenberg, N. F. Azevedo, and A. Ivask, "Propidium iodide staining underestimates viability of adherent bacterial cells," *Sci. Rep.*, vol. 9, no. 1, pp. 1–12, 2019.

[36] P. Stiefel, S. Schmidt-Emrich, K. Maniura-Weber, and Q. Ren, "Critical aspects of using bacterial cell viability assays with the fluorophores SYTO9 and propidium iodide," *BMC Microbiol.*, vol. 15, no. 1, pp. 1–9, 2015.

[37] A. C. Gerstein and J. Berman, " Candida albicans Genetic Background Influences Mean and Heterogeneity of Drug Responses and Genome Stability during Evolution in Fluconazole ," *mSphere*, vol. 5, no. 3, 2020.

[38] M. Yekani *et al.*, "Collateral sensitivity: An evolutionary trade-off between antibiotic resistance mechanisms, attractive for dealing with drug-resistance crisis," *Heal. Sci. Reports*, vol. 6, no. 7, pp. 1–10, 2023.

[39] V. Lara-Aguilar *et al.*, "Adaptation of the emerging pathogenic yeast Candida auris to high caspofungin concentrations correlates with cell wall changes," *Virulence*, vol. 12, no. 1, pp. 1400–1417, 2021.

[40] S. H. Mun *et al.*, "Synergistic antibacterial effect of curcumin against methicillin-resistant Staphylococcus aureus," *Phytomedicine*, vol. 20, no. 8–9, pp. 714–718, 2013.

[41] D. Romera, J. J. Aguilera-Correa, I. Gadea, L. Viñuela-Sandoval, J. García-Rodríguez, and J. Esteban, "Candida auris: a comparison between planktonic and biofilm susceptibility to antifungal drugs," *J. Med. Microbiol.*, vol. 68, no. 9, pp. 1353–1358, 2019.

[42] L. Sherry, G. Ramage, R. Kean, A. Borman, E. M. Johnson, and M. D. Richardson, "Biofilm-Forming Capability of Highly Virulent ," *Emerg. Infect. Dis.*, vol. 23, no. 2, pp. 328–331, 2017.

[43] M. Cuenca-Estrella *et al.*, "Multicenter evaluation of the reproducibility of the proposed antifungal susceptibility testing method for fermentative yeasts of the Antifungal Susceptibility Testing Subcommittee of the European Committee on Antimicrobial Susceptibility Testing (AFST-EU," *Clin. Microbiol. Infect.*, vol. 9, no. 6, pp. 467–474, 2003.

[44] J. L. Rodriguez-Tudela, "EUCAST definitive document EDef 7.1: Method for the determination of broth dilution MICs of antifungal agents for fermentative yeasts," *Clin. Microbiol. Infect.*, vol. 14, no. 4, pp. 398–405, 2008.

Figures

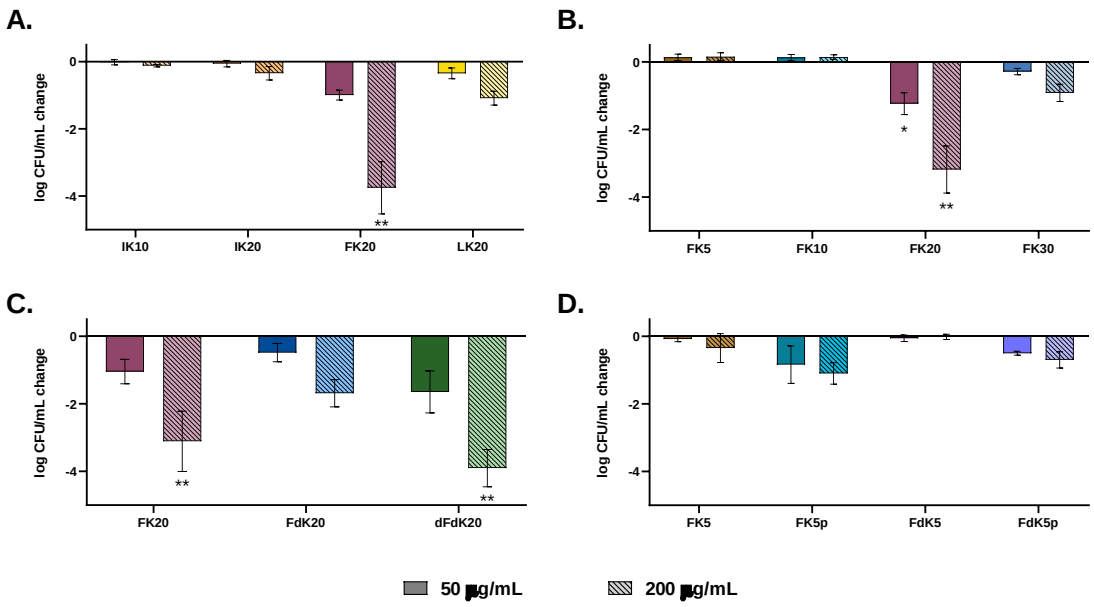

Figure 1: FK RPMs exhibit high antifungal activity against *C. auris*. *C. auris* cells were incubated with 50 or 200 µg/mL of each RPM separately for 45 min at 37°C, 200 RPM in PBS. Fungal viability was calculated by plating on YPD agar plates for CFUs. Fungicidal activity was assessed on the basis of A. amino acid composition (IK10, IK20, FK20 and LK20), B. chain length (5, 10, 20, and 30-mer FK), C. Stereochemistry (FK20, FdK20, and dFdK20), D. palmitic acid moiety addition (FK5, FK5 conjugated to palmitic acid, FdK5 and FdK5 conjugated to palmitic acid). The data are derived from three biologically independent experiments. Significance was determined with ANOVA and Bonferroni post hoc test. *$p < 0.05$; **$p < 0.01$ significance compared to control; data without symbols are not significantly different.

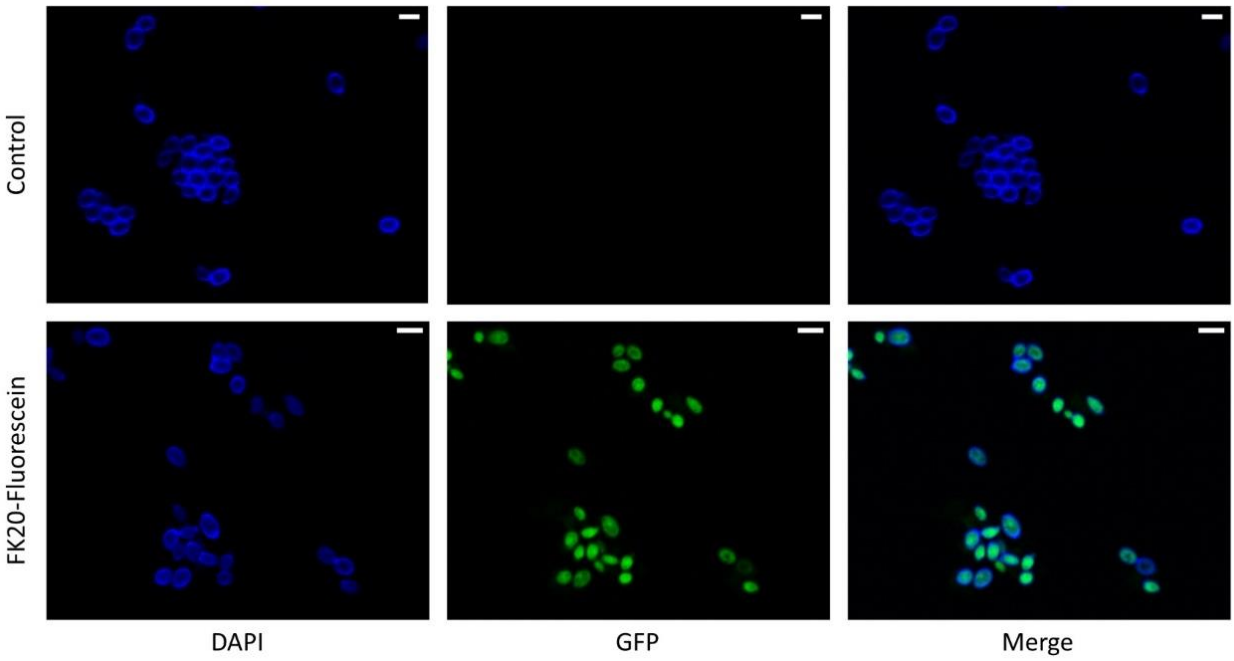

Figure 2: FK20 RPM penetrate *C. auris* cells. $5 \cdot 10^{7}$ CFU/mL of *C. auris* cells were incubated together with 200 µg/mL fluorescently labeled 20-mer FK RPM (green) for 45 min at 37ºC in PBS. Samples were stained with Calcofluor White stain (blue). Images shown were taken by confocal microscope, at a magnification of 40×. Scale bars, 5µm. Images representative of three biologically independent experiments.

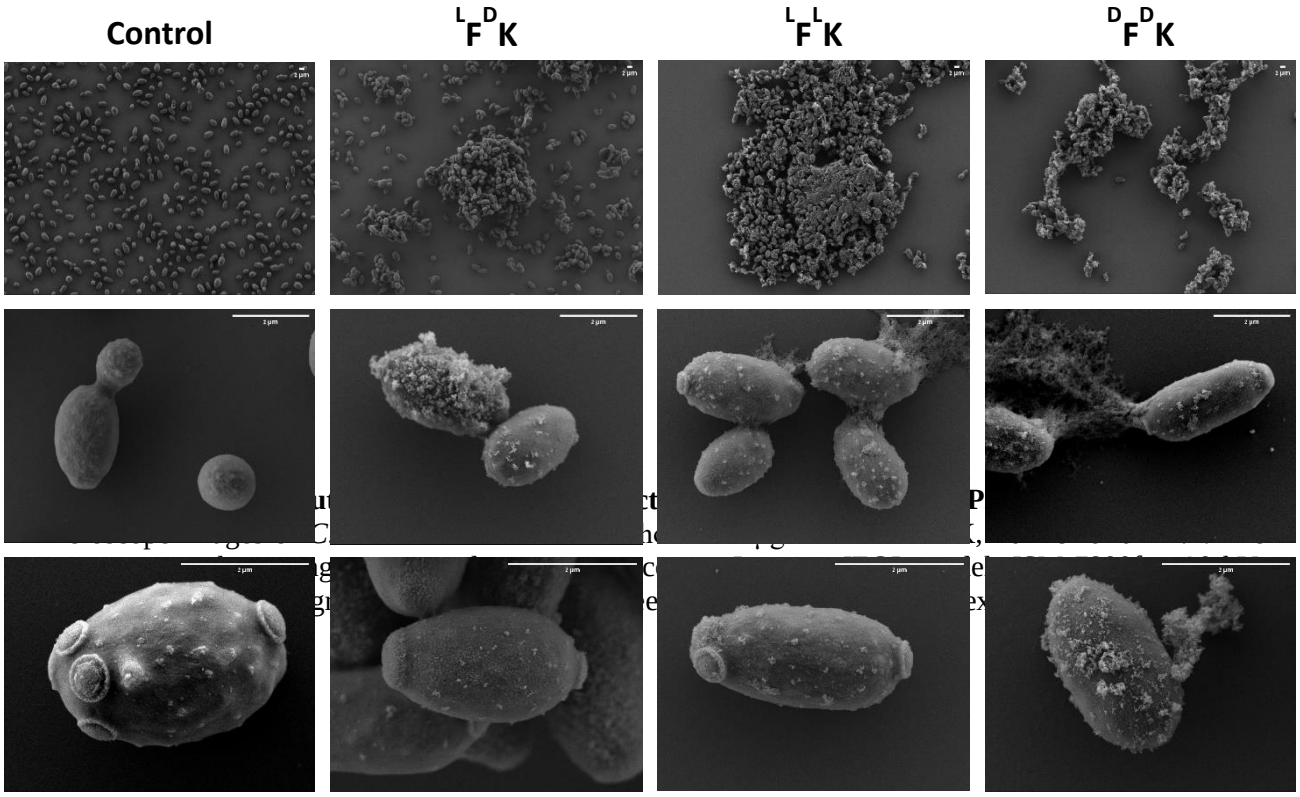

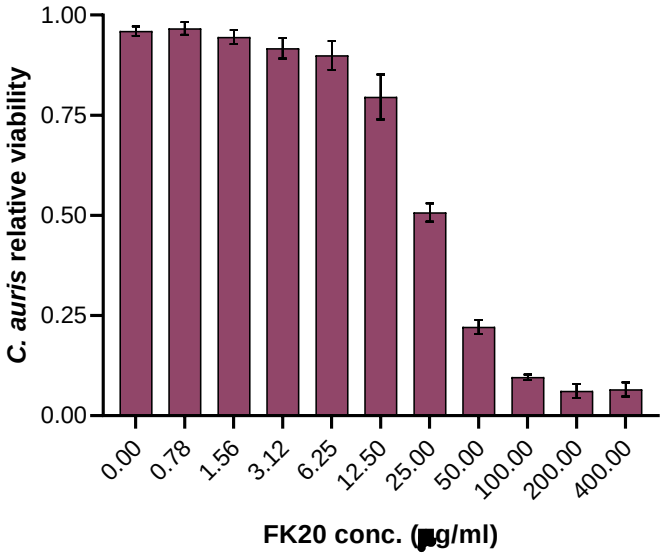

Figure 4: FK20 induce dose-dependent membrane damage in *C. auris*. *C. auris* cells were incubated with 20-mer FK RPM at concentration ranging from 0 – 400 µg/mL for 45 minutes at 37°C with continuous shaking. Membrane damage was evaluated by staining *C. auris* cells with Propidium Iodide for 20 minutes. Cell viability was determined by measuring PI fluorescence using a flow cytometer. The viability of *C. auris* was calculated as the percentage of cells remained unstained by PI. The data are derived three biologically independent experiments conducted in triplicates.

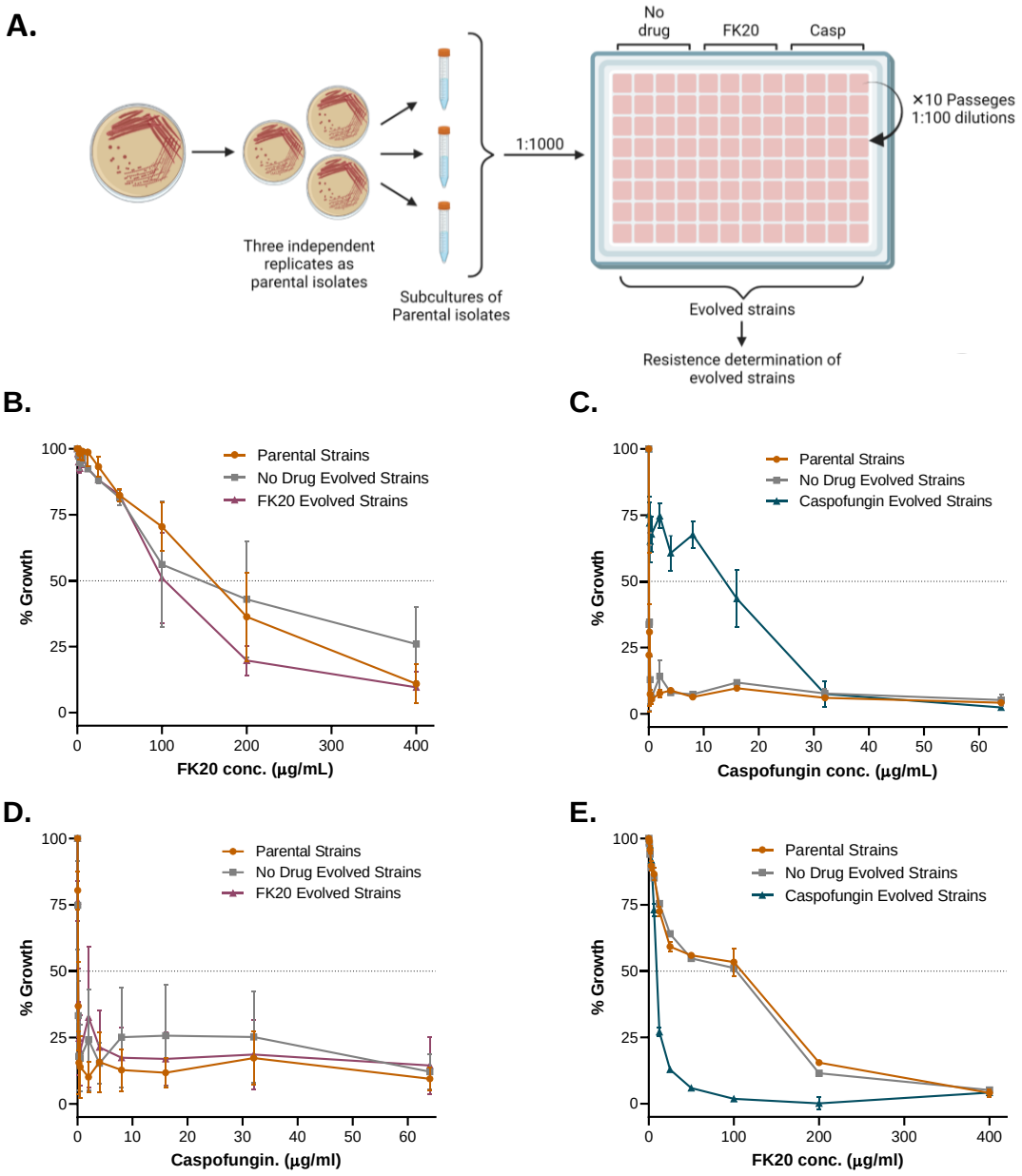

Figure 5: In vitro-experimental evolution. A. A scheme delineating the experimental evolution approach of *C. auris* in the presence of FK20 and caspofungin. The experimental evolution of *C. auris* was conducted with three independent replicates as initial parental strains to generate three independent evolved lineages. The resistance profiles of the resulting strains were assessed by determining the MIC-50 values for the parental strains, non-drug-evolved strains, and strains evolved under FK20 or caspofungin conditions. The MIC was determined using the broth microdilution method after 72 hours of incubation of *C. auris* in their respective drug environments. Growth was evaluated by measuring optical density (OD590) in the presence of incrementally increasing concentrations of either FK20 (B) or caspofungin (C). The percentage of growth was calculated by comparing the growth of treated *C. auris* cells to that of untreated cells. D-E. Collateral sensitivity of caspofungin-evolved strains with FK20 RPM (D), and FK20-evolved strains to caspofungin. Each data point represents the mean and standard error of mean calculated from three lineages in three independent experiments performed in triplicates.

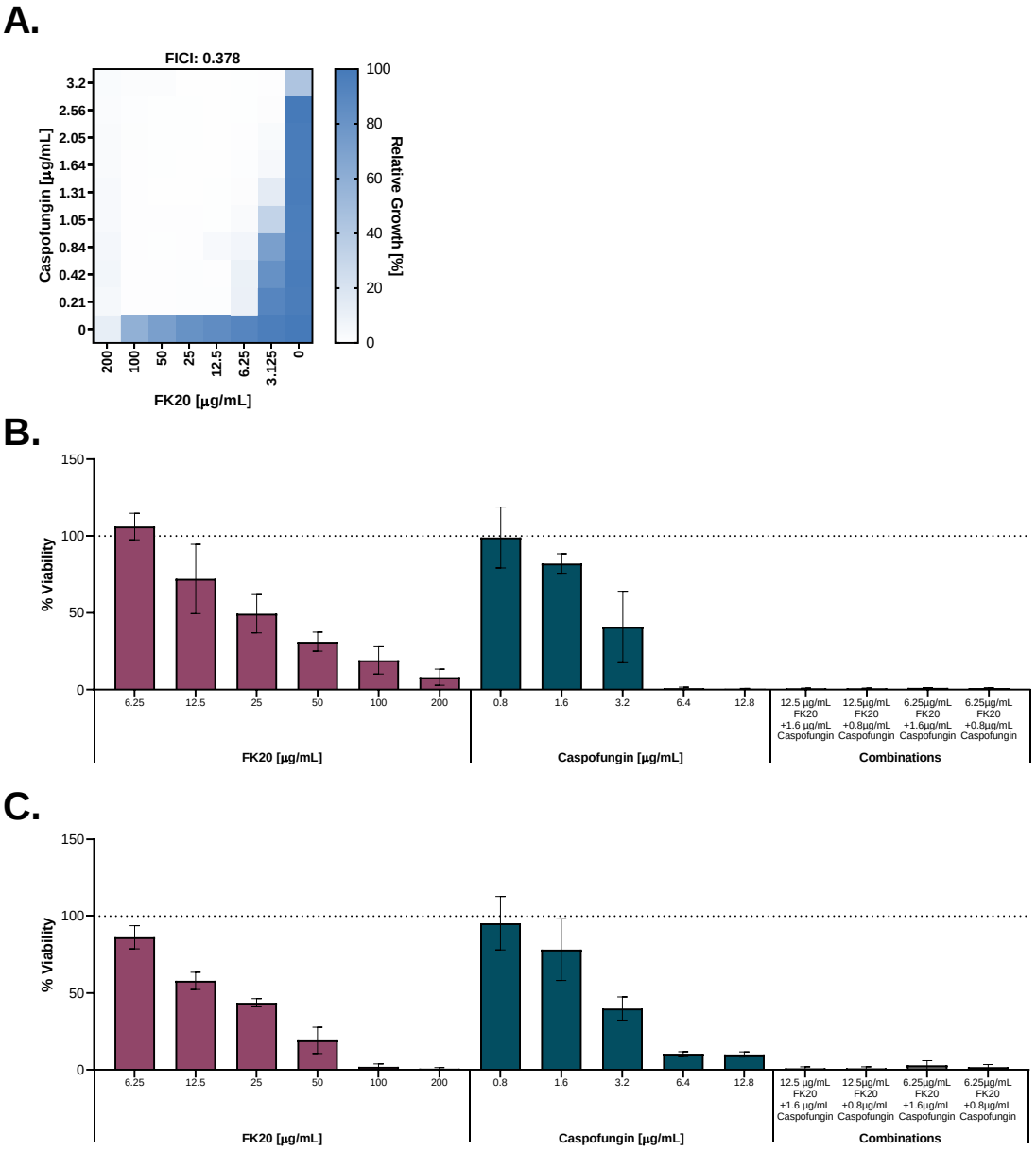

Figure 6: Synergistic effect of FK20 and caspofungin on *C. auris* biofilm formation. A. Combined effects of FK20 and caspofungin on *C. auris* cells. The Fractional Inhibitory Concentration (FICI) Index was determined using a checkerboard assay. The heat map illustrates the percentage growth of *C. auris* under various combinations of caspofungin and FK20 concentrations. B-C. Inhibition of *C. auris* biofilm formation by FK20, caspofungin, and their combination, quantified via MTT (B) and crystal violet (C) after 24 hours. FK20 and caspofungin were included in the growth medium from the beginning of the experiment. The data are derived from three biologically independent experiments conducted in six replicates. Error bars represent SEM.

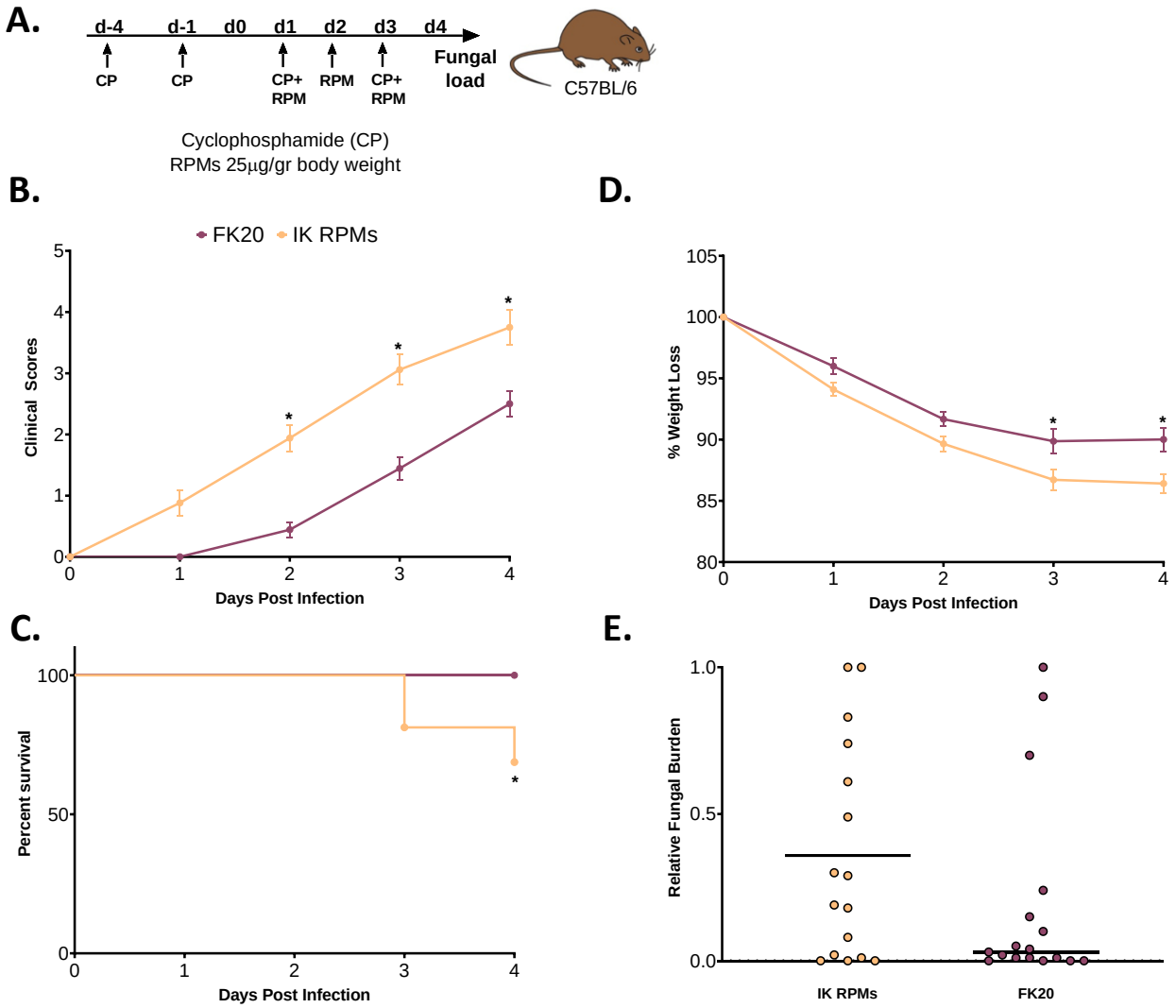

overview of the timeline of infection in a murine model of systemic candidiasis. Mice were immunosuppressed using Cyclophosphamide, infected i.v. with 1 x 10^6 CFUs of *C. auris* and treated daily i.m. with 25 µg/gr FK20 or IK RPMs 4 days post infection. B. Clinical scores, & C. Percentage weight loss representative of disease severity obtained from observations of physical activity and weight of mice infected with *C.auris* which treated with FK20 or IK RPMs. D. Percentage of mice survival. E. Fungal burden in kidneys of treated mice. Data was normalized by: $(X-X_{min})/range$, while range= $X_{max}-X_{min}$. Error bars represent SEM for n = 16 (IK RPMs) and n = 17 (FK20). Significance was determined with t test; *$p < 0.01$.

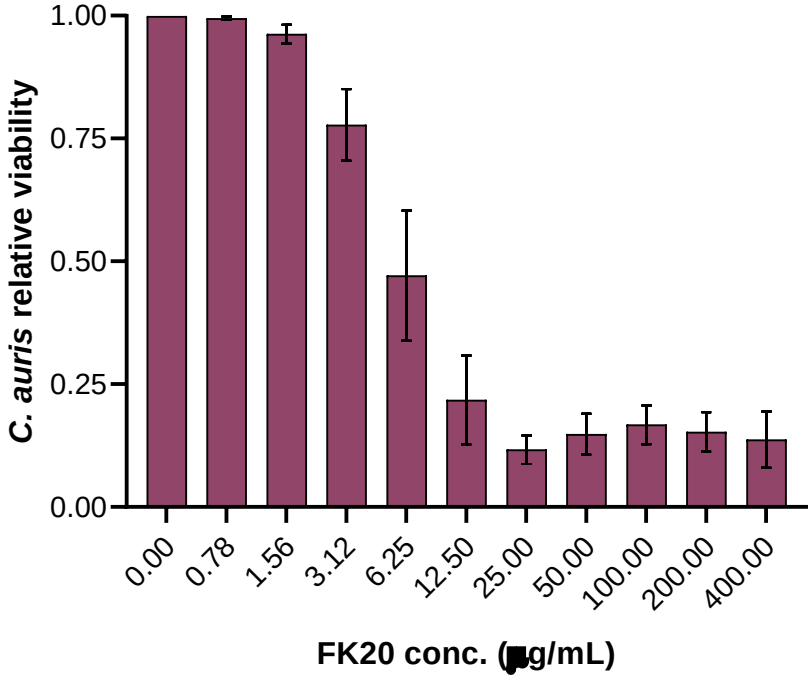

Figure S1: Membrane damage quantification by ghost dye staining. *C. auris* cells were incubated with FK20 RPM at concentration ranging from 0 – 400 µg/mL for 45 minutes at 37°C with continuous shaking. Membrane damage was evaluated by staining *C. auris* cells with Ghost dye for 20 minutes. Cell viability was determined by measuring Ghost dye fluorescence using a flow cytometer. The viability of *C. auris* was calculated as the percentage of cells remained unstained by Ghost dye. The data are derived three biologically independent experiments conducted in triplicates.

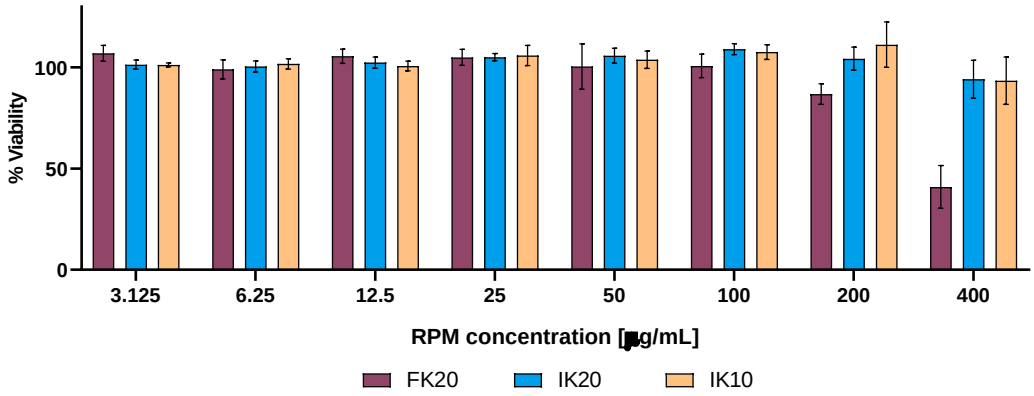

Figure S2: RPMs exhibit no cytotoxicity in cultured cells. RAW 264.7 murine macrophage cells were incubated with FK20, IK20, or IK10 for 24 hours at 37°C in a 5% CO_2 environment. Cell viability was assessed using the MTT assay, with macrophage viability expressed relative to a control group with no treatment. The data represent the mean of three biologically independent experiments, each performed in triplicate.

Test	UPW	IK10	FK20	Reference values
AST (IU/L)	246.5 ± 341.5	81 ± 187	90 ± 275	57-329
ALT (IU/L)	20 ± 38	3 ± 28	6 ± 32	22-133
ALP (IU/L)	13.5 ± 141.5	12.5 ± 110.5	12 ± 94	16-200
GGT (IU/L)	3 >	3 >	3 >	3 >

Table S1: Hematology Profiles and Blood Chemistry. A control group of Mice were administered ultra-pure water, FK20 or IK10 RPMs intramuscularly daily for four days (25 µg/gr body weight). Hematology and blood chemistry was analyzed on day four. n=5 per group.

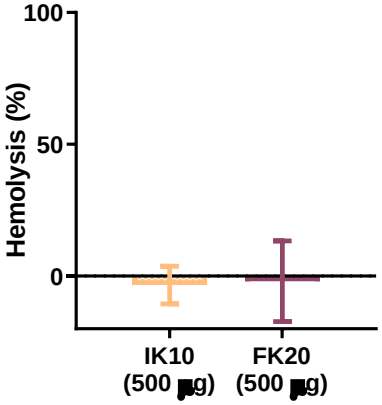

Figure S3: RPMs are not hemolytic. A control group of Mice were administered ultra-pure water, FK20 or IK10 RPMs intramuscularly daily for four days (25 µg/gr body weight). Hemolysis was analyzed on day four by direct spectrophotometric measurement at 540 nm. N=5 per groups.